A spectral analysis of Deneb (A2 Iae)[*],[**]

B. Albayrak

Ankara University, Science Faculty, Department of Astronomy and Space Sciences, 06100 Tandoğan, Ankara, Turkey
(albayrak@astro1.science.ankara.edu.tr)

Abstract. This study presents a detailed model atmosphere abundance analysis of Deneb which was performed using Kurucz LTE ATLAS9 model atmospheres. The atmospheric parameters were determined from Mg I/II and Fe I/II equilibrium, and by fitting the H_γ profile and optical region spectrophotometry. The compromise values which best satisfy these criteria are T_{eff} = 9000 K and log g = 1.45. The Mg I, Mg II, Si II, Ti II, Cr II, Fe I, and Fe II lines yield microturbulences of 3.60, 6.50, 8.50, 8.00, 11.90, 3.60, and 10.40 km s^{-1}, respectively. An average microturbulence of 7 km s^{-1} was used for the other atomic species.

From a comparision of the synthetic spectrum with the observations, the best value for the rotational velocity is $v \sin i$ = 25 km s^{-1}, and for the macroturbulent velocity is ζ = 14 km s^{-1}, which are similar to those of some earlier derived values. Also, the individual spectrograms have a range of radial velocity variation of $\sim$ 15 km s^{-1} which is approximately equal to macroturbulent velocity. These values of the macroturbulence and the range of radial velocity variation are close to the sum of the amplitudes (10.44 km s^{-1}) of all the pulsation periods found by Lucy (1976), who also suggested that the surface motions of the atmosphere of Deneb can be identified with macroturbulence.

Deneb showed a definite helium underabundance with a well determined He/H value = 0.071. The CNO values (C being mildly deficient, N being in moderate excess, and an O being slightly deficient) are consistent with the mixing of the CNO-cycled products into the surface layers from the processed materials presumably dredged-up from the interior. Aluminium is mildly deficient by $\sim$ 0.24 dex with respect to solar value, while sulfur is moderately underabundant by $\sim$ 0.43 dex in Deneb. Mg and Si have the solar abundances. The metal abundances (Ca to Ni) tend to be greater than solar except for Sc which is slightly deficient. The heavy elements abundances (Sr, Y, and Zr) are all greater than solar. These abundance patterns conform to the common tendency seen with other normal Population I A su-

pergiants found by Venn (1995a). The rare-earth elements (Ba, La, and Eu) which have been unexplored in other Galactic early A-type supergiants are significantly overabundant relative the Sun.

1. Introduction

Deneb is the prototype of the early A-type supergiants, which are among the most luminous stars in the Milky Way and in other spiral galaxies. It is relatively sharp-lined and unreddened. The literature concerning Deneb and similar supergiants is both extensive and in depth. Two of the most cited papers are by Groth (1961), who made a detailed analysis of Deneb's atmosphere, and by Lucy (1976), who found radial velocity variations in 16 modes with periods between 6.9 and 100.8 days and with amplitudes from 0.29 to 1.02 km s^{-1} from a Fourier analysis of Paddock's (1935) data. Lucy concluded that these broad range of periodicities in pulsations represent the macroturbulence in the atmosphere of Deneb.

Buscombe (1951), Chadeau (1955), Groth (1961), Taffara (1966), Zverko (1971), Samedov (1993), and Takeda et al. (1996) have studied the photospheric chemical composition of Deneb. Groth (1961) concluded that the metal abundances in the atmosphere of Deneb are on average $\sim$ 0.3 dex greater than solar. Samedov (1993) found a nitrogen excess of $\sim$ 0.11 dex and a carbon deficiency of $\sim$ 0.3 dex while the other elements (He, O, Mg, Si, Sc, Ti, V, Cr, Fe, Ni, and Sr) have approximately the solar values. According to Takeda et al. (1996)'s NLTE results, carbon and oxygen have deficiencies of $\sim$ 0.8 and $\sim$ 0.4 dex, respectively. The other elements (N, Na, and S) show a mild excess of 0.3 to 0.4 dex, and He has nearly the solar abundance. Especially when comparing Groth (1961)'s results to more recent analyses, we must remember that there have been substantial changes in the atomic oscillator strengths for some atomic species in the last 35 years. Most of the differences in the derived abundances between this study and those of other authors are due to differences in the spectrograms used, analy-

---

sis tools, atomic data and model atmospheres. A new detailed analysis for Deneb was performed for the following reasons:

1. Very high signal-to-noise ratio (S/N = 500) spectroscopic observations are now possible with modern electronic devices such as CCDs or Reticons while older studies used non-linear photographic plates with signal-to-ratios of typically 25 or 50 for bright stars. The combination of these devices with a high resolution spectrograph enables analysis of profiles of even faint lines with high accuracy.

2. The scattered light correction of 3.5% (Gulliver et al. 1996) was used in this analysis while the previous studies did not include any and hence contain systematic errors.

3. VLINE (Hill & Fisher 1986) allows much better spectrograms measurements than with earlier techniques. Furthermore, this study has found many more identified lines (especially weaker features, see Albayrak et al. 2000) and also new atomic species for Deneb with Dominion Astrophysical Observatory (DAO) spectrograms.

4. Reliable atomic data are now available for many more atomic and ionic lines than a decade or so ago.

5. The model atmospheres were calculated using the ATLAS9 code of Kurucz (1995) with the usual assumptions of LTE, hydrostatic equilibrium, plane parallel geometry and solar metallicity. ATLAS9 also includes a detailed description of the opacity due to metal line-blanketing. ATLAS9, a modern code with the best available atomic data, allows one to integrate the curve-of-growth through the atmosphere better than previous models. Previous analyses of Deneb used either the curve-of-growth method (Buscombe 1951; Chadeau 1955; Taffara 1966; Zverko 1971) or model atmospheres without metal line-blanketing (Groth 1961). Only Samedov (1993) investigated Deneb by the use of Kurucz (1979)'s model atmospheres. He analyzsed one 4 Å mm^{-1} Kodak IIIaJ spectrum.

6. For the first time, optical spectrophotometric observations of Deneb have been used to determine its atmospheric parameters. We also used synthetic spectra to determine macroturbulence.

2. The spectra

Reticon and CCD DAO spectrograms, with a resolution of 0.072 Å were used: they covered 67 and 63 Å, respectively, in the region $\lambda\lambda 3830 - 5212$. Using the exposures of an incandescent lamp, the exposures were flat fielded. A central stop removed light from the beam as does the secondary mirror of the telescope. The spectra were rectified using the interactive computer graphics program REDUCE (Hill & Fisher 1986). In a few regions, we used single spectra with signal-to-noise ratios of about 750. These values were found by measuring line free continuum regions. Often the spectra for a given region are co-added (Hill & Adelman 1986) to increase the signal-to-noise ratio to 900 or more. The lines found, their wavelengths, line widths, line depths, and probable identifications will be present as a spectral atlas (Albayrak et al. 2000). This should be a useful guide for other A-type supergiants.

## 3. Atmospheric analysis

3.1. Atmospheric parameters

Most published results concerning the effective temperature and surface gravity for Deneb are in the range of T_{eff} = 10080 to 7635 K, and log g = 2.5 to 1.0 dex, respectively (see Albayrak 1999). To determine the atmospheric parameters of effective temperature and surface gravity (T_{eff}, log g), one can compare Balmer line profiles (especially H_β, H_γ, H_δ) and the continuous energy distribution of a star derived from measurements of the stellar flux by means of narrow-band photometric scans. This gives a model whose products simultaneously fit both quantities. Often one can find a locus of acceptable fits as a function of T_{eff} and log g. These Balmer lines have been routinely used as the slope of the continuum is not locally great. Telluric lines are few or minimal near H_γ and H_δ and can be accurately removed from H_β. Furthermore, these lines are not as prone as H_α to having emission line components. The effect of interstellar reddening must be removed from the observed energy distribution before comparison with the model fluxes.

For Deneb the H_γ profile is derived from a 2.4 Å mm^{-1} DAO Reticon spectra (W48904016), and agrees with a 20 Å mm^{-1} Reticon spectra (W48921671). The 2.4 Å mm^{-1} exposure was used as it has higher resolution. A 3.5 percent scattered light correction (Gulliver et al. 1996), was applied before comparision with the predictions of ATLAS9 model atmospheres (Kurucz 1995). I used SYNTHE (Kurucz & Avrett 1981) to calculate the synthetic spectra of the H_γ region for fitting the wings of this line.

The interstellar extinction law of Schild (1977) was used to correct the stellar spectrophotometric data which was primarily that of Schild et al. (1971), as converted to the Hayes-Latham (1975) calibration of Vega from Breger (1976), and secondly the optical energy distribution from Alekseeva et al. (1996). For stars similar to Deneb, the energy distribution depends mainly on T_{eff} and secondarily on log g.

Another way of determining effective temperature and surface gravity pairs is by demanding *ionization equilibrium*, where equal abundances are derived from two different ionic states of an element. Such determinations may be possible for several elements. Lines of Mg I and Mg II used as NLTE effects, are predicted to be small for lines of both species of Mg in Vega, which is a main-sequence A0-type star (Gigas 1988), in Procyon which is a subgiant star (F5 IV-V) (Mashonkina et al. 1995), and also in A-type supergiants (Venn 1995a), which makes Mg an ideal element for this analysis.

In addition, lines of Fe I and Fe II were used. Gigas (1986) notes that the NLTE abundance corrections for Fe I lines are of the order of 0.32 dex and for Fe II lines, are between 0.02 and 0.18 dex in Vega. However, the use of the NLTE corrections for Fe I and Fe II means the derived abundances agree more poorly than those without the correction. Perhaps the problem is that Vega is a fast rotator seen pole-on (Gulliver et al. 1994). Hence there is about a 500 K effective temperature difference between the hotter polar and cooler equatorial regions. Furthermore, the model atom may not be sufficiently complete. As it is
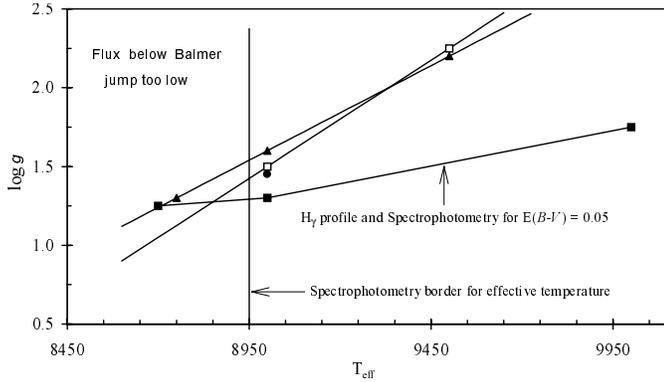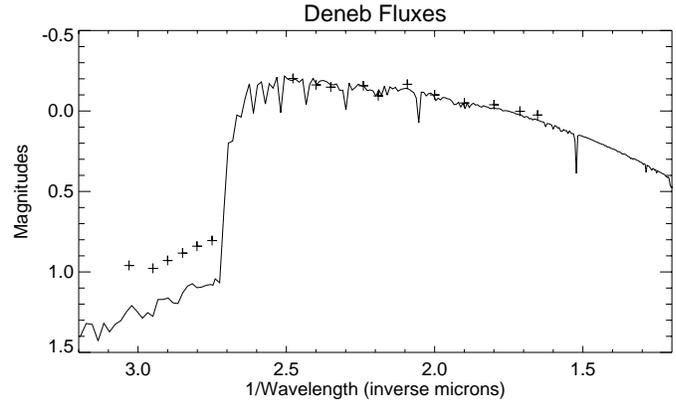
Fig. 1. A T_{eff}-log g diagram (a Kiel Diagram) for Deneb. The results from three methods are shown as follows: the closed triangles and open squares represent data determined from Mg I/II or Fe I/II ionization equilibrium, respectively, closed squares are from fitting the H_γ profile and the spectrophotometry for E(B-V) = 0.05. The vertical line at the 8950 K is the spectrophotometry border for the minimum T_{eff} value. The adopted model atmosphere parameters are marked with a closed circle.


Fig. 2. The optical region energy distribution of Deneb which includes a correction for E(B-V) = 0.05 (pluses), compared with the predictions of an ATLAS9 model with solar composition, $T_{\mathrm{eff}} = 9000$ K and log g = 1.45 (solid line). The observational data are from Schild et al. (1971). The observed continuum energy distribution in the Paschen continua shows a fairly good agreement with our model flux.

unclear whether to apply Gigas' NLTE corrections, they were not applied.

The locus of the atmospheric parameters derived from magnesium *ionization equilibrium* for log ϵ(Mg I) = log ϵ(Mg II), iron ionization equilibrium for log ϵ(Fe I) = log ϵ(Fe II) and from fitting theoretical H_γ profiles to observed ones, are shown in Fig. 1 (T_{eff} vs. log g, a Kiel Diagram of Deneb) as well as a comparison of spectrophotometry and its predicted fluxes for E(B-V) = 0.05. This is a very good visualization tool, since it allows one to view the relative position of solutions from the different methods. As seen in this diagram, the atmospheric parameters for Deneb, the intersection of Mg ionization equilibrium locus and Fe ionization equilibrium locus lead to T_{eff} = 9325 K and log g = 2.00. On the other hand, the intersection of the H_γ locus and the Mg ionization equilibrium (Mg I/II) locus on the temperature-gravity plane, yields T_{eff} = 8700 K, log g = 1.25 while the convergence point of H_γ locus and Fe ionization equilibrium (Fe I/II) locus leads to T_{eff} = 8850 K, log g = 1.26. However, spectrophotometry requires that (as mentioned below) the effective temperature be greater than 8950 K due to the observed optical UV flux (i.e. that below Balmer jump). Thus, our adopted values T_{eff} = 9000 K and log g = 1.45 are a compromise. At the cost of making the other criteria worse, one can get a better fit. If sphericity effects are large, a model in which they are included will have a larger Balmer jump than a plane-parallel model with similar effective temperature and surface gravity (see Kubat 1996). An average microturbulent velocity of 8 km s^{-1} was used for the model atmosphere calculation (see below).

Use of the spectrophotometric flux values permits one to make a good determination of T_{eff}. However, it must be corrected for any interstellar reddening. To simultaneously fit the spectrophotometry and the H_γ profile, a value E(B-V) = 0.04 or greater is required. The derived locus in the T_{eff} and log g plane is a function of E(B-V). Increasing E(B-V) to 0.09 makes

compromise solutions near 9000 K difficult. E(B-V) = 0.05 resulted in the best flux fits, and so was adopted. In the portion of the spectrum which was examined, the only emission line that was found was in the core of Hα. Thus almost all photometric magnitudes and the spectrophotometric fluxes are unaffected by emission lines.

In the Geneva system (B2-V1) = –0.029 for Deneb (Rufener 1976). Meynet & Hauck (1985) found the intrinsic Geneva colours for an A2 Ia supergiant to be –0.085. Thus, the color excess is E(B2-V1)= 0.056 which corresponds to a Johnson E(B-V) = 0.063. Gray (1992) estimated in the Strömgren photometric system, a reddening value of E(b-y) = 0.05 which corresponds to a Johnson E(B-V) = 0.072 (Venn 1995a). The mean of Lanz (1986) and Mermilliod (1991)'s values for Deneb's (B-V) colour is 0.09. Fitzgerald (1970) states that the intrinsic (B-V) colours for an A2 Ia supergiant is 0.05. In this case, its colour excess E(B-V) is 0.04 in the Johnson photometric system. Hence photometry suggests that the reddening E(B-V) is between 0.04 and 0.07.

Fig. 2 shows the agreement of the observed optical energy distribution from Schild et al. (1971) with the predictions of the adopted solar composition model, T_{eff} = 9000 K and log g = 1.45, for Deneb. The observed continuum energy distribution in the Paschen continua is generally in fairly good agreement with our model flux while the computed flux is below that observed in the Balmer continua. It is also possible to fit to the Balmer continua at the same time (see the T_{eff} and log g values in Fig. 1). That the observed values near Hα are slightly too bright may be a systematic error or indicate that additional line opacities are needed. There is a tendency for some normal and chemically peculiar stars to show a similar effect (Adelman et al. 1995). We compare in Fig. 3 the optical energy distribution of Schild et al. (1971) and Alekseeva et al. (1996). There are no major differences between their spectrophotometric data. The first value for the Schild et al.'s data is probably not correct.
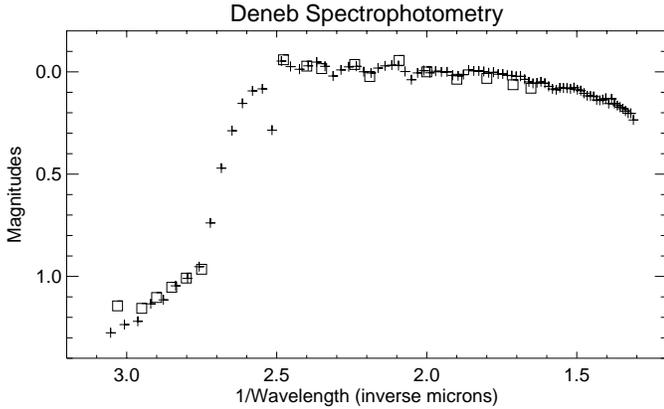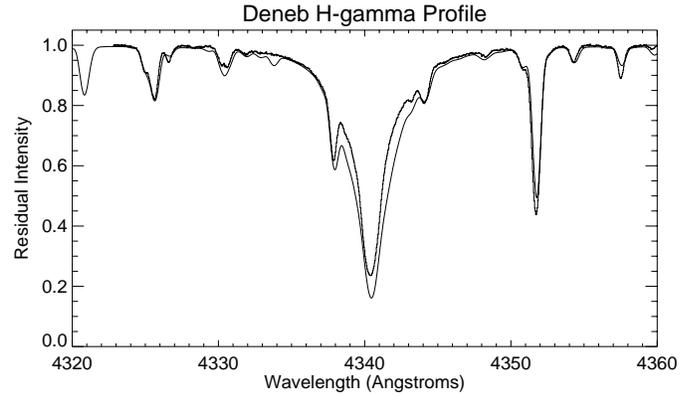
Fig. 3. The comparison of spectrophotometric data of Deneb that are from Schild et al. (1971) (open squares) and Alekseeva et al. (1996) (pluses). Otherwise, the same as in Fig. 2.

Fig. 4. The observed H_γ profile of Deneb which is corrected for 3.5% scattered light (upper heavy line), is compared with the theoretical profile of the adopted $T_{\rm eff}$ = 9000 K, log g = 1.45 and solar composition model atmosphere (lower thin line). It shows a very good agreement in the wings.

The observed H_γ profile for Deneb and the predicted theoretical profile for the adopted model atmosphere are shown in Fig. 4 to help visualize the fits to the core and line shoulder. As seen in this figure, the model predictions for Deneb using $T_{\rm eff}$ = 9000 K and log g = 1.45 exhibit a good match with the observed profile which have been corrected for the 3.5% scattered light, in the blue wing. In the line core where the assumption of Local Thermodynamic Equilibrium (LTE) breaks down, the agreement is poor.

3.2. Abundance analysis

Programs SYNSPEC (Hubeny et al. 1994) and WIDTH9 (Kurucz, private communications) were used to determine the helium and metal abundances, respectively. Significantly blended lines were not used in the abundance analysis. Generally, lines have also been excluded for a given species if the standard deviation of the computed abundances is greater than 0.3 dex.

The microturbulent velocities were obtained by requiring that there is no dependence of derived abundances on the equivalent widths (ξ_1) and that the standard deviation of the means were minimized (ξ_2). We found 3.60 km s^{-1} from 7 lines of Mg I, 6.50 km s^{-1} from 9 lines of Mg II, 8.50 km s^{-1} from 12 lines of Si II, 8.00 km s^{-1} from 70 lines of Ti II, 11.90 km s^{-1} from 49 lines of Cr II, 3.60 km s^{-1} from 118 lines of Fe I and 10.40 km s^{-1} from 155 lines of Fe II (Table 1). Thus there are significant differences between microturbulent velocities found for neutral and singly ionized magnesium and iron lines and also a clear variation of microturbulence with species. Also, Mg I and Fe I yield a significantly smaller microturbulent velocity than other species. These differences do not seem to be the result of a defect in our approach. The simplest interpretation of these results are that they may represent a stratification effect and may reflect the existence of a velocity gradient in the atmosphere of this star. Similar results have been reported for Deneb by Rosendhal (1970), Zverko (1971), and Aydın (1972) (see also Table 5). Hence the microturbulent velocity in the atmosphere of Deneb may not be constant with optical depth. Throughout the line forming region of the atmosphere in Deneb, it has a mean value of 7.5 km s^{-1} from Table 1. Thus, we assumed on the average (depth-independent) microturbulent velocity value of 8 km s^{-1} for the model atmosphere calculation as this gives a consistency with the available opacity distribution functions. For the subsequent abundance analysis for all species not showed in Table 1, 7.0 km s^{-1} was used.

The helium/hydrogen (He/H) ratio is a key parameter in stellar abundance analyses as well as in cosmology and stellar evolution. Eight relatively unblended He I lines were selected from those lines observed in Deneb's spectrum. Other observed He lines were too weak or too blended. The line profiles were calculated for a variety of He/H ratios with the adopted solar helium model atmosphere using the program SYNSPEC. For comparison with the observations the theoretical line profiles were convolved with the rotational velocity and the instrumental profile. For each line the He/H value is that for the computed profile which best matches the observations. The average of these values is He/H = 0.071 ± 0.008 (Table 2).

Fig. 5 shows a good but not perfect match of the He I λ4771 line with Deneb. Program SYNSPEC as configured did not include metal blending lines. The abundance of He turned out to be slightly less than solar (log ϵ(He) = 10.85 ± 0.01). A difference of –0.15 dex is a definite underabundance as the He/H value is well determined, better than most metal abundances.

The metal line damping constants are based on the data of Kurucz & Bell (1995). Table A.1 (in the appendix), contains the multiplet number (Moore 1945) for each line, the laboratory wavelength (in Å), the logarithm of the gf-value and its source, the equivalent width (mÅ) as observed, and the deduced abundance. The scatter of the individual abundances about the mean are given for each atomic species, whenever appropriate. A factor of 2 in abundances corresponds to 0.30 dex which is generally used as a criteria for significant differences. To convert log N/N_T values to log N/H values the average He/H value of Deneb was used. The final abundance results are presented in Table 3 as unweighted average abundances per species. Abundances are

Table 1. The derived microturbulent velocities for each species.

Species	Number of lines	ξ_1 (km s^{-1})	log N/N$_T$	ξ_2 (km s^{-1})	log N/N$_T$	adopted ξ (km s^{-1})	gf values$^{(\star)}$
Mg I	7	3.50	-4.17 ± 0.19	3.70	-4.20 ± 0.19	3.60 ± 0.1	FW, JK, KX and WS
Mg II	9	6.40	-4.54 ± 0.13	6.60	-4.55 ± 0.13	6.50 ± 0.1	FW, KP and WS
Si II	12	8.30	-4.62 ± 0.20	8.70	-4.65 ± 0.19	8.50 ± 0.2	KG, KP, LA, SG, and WS
Ti II	70	8.00	-7.03 ± 0.23	8.10	-7.03 ± 0.23	8.00 ± 0.1	KX and MF
Cr II	49	11.60	-6.31 ± 0.29	12.20	-6.31 ± 0.29	11.9 ± 0.3	KX and MF
Fe I	118	3.50	-4.26 ± 0.29	3.70	-4.27 ± 0.29		KX and MF
	95	3.50	-4.28 ± 0.29	3.60	-4.28 ± 0.29	3.60 ± 0.2	only MF
Fe II	155	10.40	-4.56 ± 0.20	10.50	-4.56 ± 0.20		KX and MF
	41	10.20	-4.54 ± 0.16	10.50	-4.56 ± 0.16	10.40 ± 0.2	only MF

Notes$^{(\star)}$: FW = Fuhr & Wiese (1990), JK = Jönsson et al.(1984), KP = Kurucz & Peytremann (1975), KG = Kurucz (guess – 1995), KX = Kurucz (1995), LA = Lanz & Artru (1985), MF = Fuhr, Martin & Wiese (1988) and Martin, Fuhr & Wiese (1988), SG = Schulz-Gulde (1969), and WS = Wiese, Smith & Glennon (1966) and Wiese, Smith & Miles (1969).
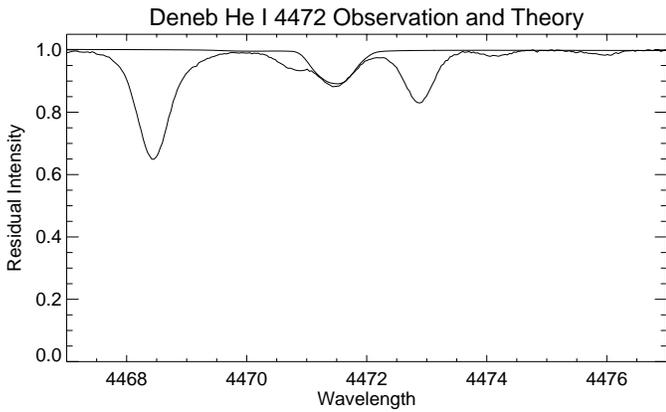
Fig. 5. The representative comparison the observed (lower line) and calculated (upper line) line profile of He I λ4471 illustrates a fairly good agreement.

Table 2. He/H ratios of Deneb.

Line (λ in Å)	He/H
4009	0.06
4026	0.06
4120	0.07
4169	0.08
4437	0.07
4471	0.08
4713	0.07
4921	0.08
Average = 0.071 ± 0.008	

Table 3. Comparision of derived and solar abundances (log ϵ).

Species	Sun*	Deneb	[X]	Number of lines
He I	(11.00)	10.85 ± 0.01	–0.15	8
C I	8.55	8.21 ± 0.20	–0.34	3
C II	8.55	8.94	+0.39	1
N I	7.97	8.88 ± 0.28	+0.91	5
N II	7.97	8.31 ± 0.28	+0.34	2
O I	8.88	8.63 ± 0.30	–0.25	4
Mg I	7.58	7.69 ± 0.26	+0.11	7
Mg II	7.58	7.51 ± 0.14	–0.07	9
Al I	6.47	6.25 ± 0.13	–0.22	2
Al II	6.47	6.21	–0.26	1
Si II	7.55	7.40 ± 0.21	–0.15	12
S II	7.33	6.90 ± 0.25	–0.43	10
Ca II	6.36	6.79	+0.43	1
Sc II	3.17	2.95 ± 0.18	–0.22	3
Ti II	5.02	5.00 ± 0.23	–0.02	70
V II	4.00	4.12 ± 0.28	+0.12	21
Cr I	5.67	6.06 ± 0.19	+0.39	6
Cr II	5.67	5.72 ± 0.29	+0.05	49
Mn I	5.39	5.36	–0.03	1
Mn II	5.39	5.60 ± 0.27	+0.21	22
Fe I	7.50	7.74 ± 0.30	+0.24	118
Fe II	7.50	7.57 ± 0.27	+0.07	155
Fe III	7.50	6.92	–0.58	1
Ni I	6.25	6.48 ± 0.21	+0.23	4
Ni II	6.25	6.24 ± 0.08	–0.01	4
Sr II	2.97	3.28 ± 0.09	+0.31	2
Y II	2.24	3.03 ± 0.22	+0.79	5
Zr II	2.60	3.41 ± 0.20	+0.81	12
Ba II	2.13	2.88	+0.75	1
La II	1.17	2.81	+1.64	1
Eu II	0.51	2.48	+1.97	1

* The solar abundances are from Grevesse et al. (1996)

given on the usual scale, [X] = log ϵ(X)$_{star}$ − log ϵ(X)$_\odot$ for any abundance quantity X, and log ϵ(X) = log (N$_X$/N$_H$) +12.0 for absolute number density abundances. The adopted solar abundances are from Grevesse et al. (1996).
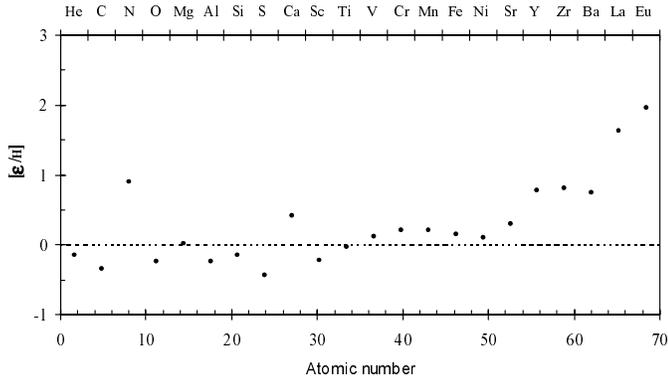
As seen in Table 3, the Mg I and Mg II lines and the Fe I and Fe II have abundance results with 0.17 dex differences in the Mg I/II and Fe I/II ionization equilibrium, a result of the compromised nature of the adopted model. The ionization equilibria of these two elements were used to determine the effective temperature and gravity of Deneb (see earlier discussion). Other elements which include C, N, Al, Cr, Mn, and Ni, were also observed in more than one ionic state but were not employed in the determination of the atmospheric parameters.

Fig. 6. Abundances determined in this analysis for Deneb compared to solar abundances.

Table 4. Derived rotational velocity values for Deneb.

Line (λ)	Species	Equivalent width (mÅ)	$v \sin i$ (km s^{-1})
4348.393	Mn II	8.7	24.8
4456.632	Ti II	8.8	27.2
4478.644	Mn II	10.2	28.4
4544.018	Ti II	9.4	26.6
4544.144	Ti II	13.9	27.1
4552.406	S II	8.8	27.0
4593.792	Fe II	13.1	26.1
			Average = 26.7 ± 1.1

For C II, the only line examined, results in an abundance very different from C I. Abundances from N I and N II lines do not agree. The N I abundances are derived from five lines and yield abundances that are in good agreement with each other. But the N II abundances are from only two lines. Also, the N I abundance are greater than the N II abundance by 0.57 dex. The aluminium abundance has been determined from Al I and Al II lines which yield abundances in excellent agreement even though the Al II abundance is derived from only one line. The Cr I abundance tends to be greater than the Cr II abundance by 0.34 dex. For Cr, a similar trend was found by Venn (1995a) for A-type supergiants. The abundances from Mn I and Mn II lines do not agree well. The Mn I abundance in this analysis is from only one line. It is in the range seen from Mn II lines. The abundances derived from four lines each of Ni I and Ni II agree to within the error limit. The discrepancy between Ni species is similar to those found for Mg and Fe species.

The abundances of carbon, nitrogen, oxygen (CNO), sulfur, calcium, yttrium, strontium, zirconium, barium, lanthanum and europium are quite different from solar in Deneb. The nitrogen abundance is significantly in excess, amounting to ~ 0.63 dex, and the carbon and oxygen seem to be deficient by ~ 0.34 and 0.25 dex, respectively. The aluminium is mildly deficient by ~ 0.24 dex while sulfur is moderately underabundant by ~ 0.43 dex. The abundances of the Mg and Si are the same as for the Sun within the error limits.

In general, the metal abundances (Ca to Ni) tend to be greater than solar except Sc which is perhaps slightly underabundant for Deneb. The Ca II abundance is from only one line, $\lambda 3933$ and yields an appreciable overabundance. Also, Mn I and Fe III with only one line each yields, results that are smaller than the average abundances from other species of the element. If these lines are ignored, then the Mn and Fe abundances are slightly greater than solar. The differences between the solar and Deneb's abundances for Sc, Ti, V, Cr, Mn, Fe and Ni are –0.22, –0.02, +0.12, +0.22, +0.09, +0.15 and +0.11 dex, respectively. The heavy elements abundances, Sr, Y, and Zr are all larger than solar amounting to 0.31, 0.79, and 0.81 dex, respectively. Ba, La and Eu abundances in Deneb are based on only one line. The Ba line gave a significant overabundance of 0.75 dex while the

La and Eu lines suggest a large overabundance by a factor of 6 relative to the Sun. The Europium abundance is determined from the line of $\lambda 4129.73$ which has a large hyperfine structure. But for a 5 mÅ line this should not be of importance in determining the abundance. Fig. 6 shows the difference between the derived abundances for Deneb and the Sun.

## 4. The macroturbulent and the rotational velocities

Rotationally broadened profiles were fitted through the weak metal lines of Deneb, while Gaussian profiles were fitted through stronger lines. Strong clean metal lines were found to be symmetric as expected by Lamers & Achmad (1994). An initial estimate of the rotational velocity based on lines thought to be non-blended near Mg II $\lambda 4481$ is 26.7 km s^{-1} (see Table 4).

To determine the macroturbulence and to refine the rotational velocity, a synthetic spectrum for the $\lambda\lambda 4490–4550$ region was calculated with the model for Deneb using the program SYNTHE (Kurucz & Avrett 1981). For comparing the synthetic with the observations, a correction for scattered light 3.5% of the continuum level (Gulliver et al. 1996) was used. The calculated synthetic spectrum with macroturbulent and rotational velocities as input parameters, was matched to the rectified (normalized) observations. The values of macroturbulent and rotational velocities were changed until an optimal match was found: $v \sin i = 25$ km s^{-1} and $\zeta = 14$ km s^{-1}. The derived rotational velocity value is in reasonable agreement with 30 km s^{-1} found by Abt & Morrell (1995). More recently, Verdugo et al. (1999) found 43 km s^{-1} which includes also a macroturbulence broadening effect from Mg II $\lambda 4481$. Also, the macroturbulent velocity is in good agreement with De Jager et al. (1984)'s value of 14.2 km s^{-1} and Boer et al. (1988)'s value of 14 km s^{-1}.

Figs. 7 and 8 show some sample regions from a synthetic spectrum for the entire spectral region $\lambda\lambda 3827–5212$. In general, the spectra thus computed, agree well with that observed (see also Albayrak 1999). From inspection of these figures, many observed features have a computed counterpart so that discrepancies arise from lines missing in the synthesis. The observed features at some wavelengths are stronger than the computed ones while sometimes the computed line is stronger than observed one. Many of these problems are due to errors in the oscillator strengths and imply modest corrections for a much better fit. Thus, the derived parameters for Deneb's atmosphere
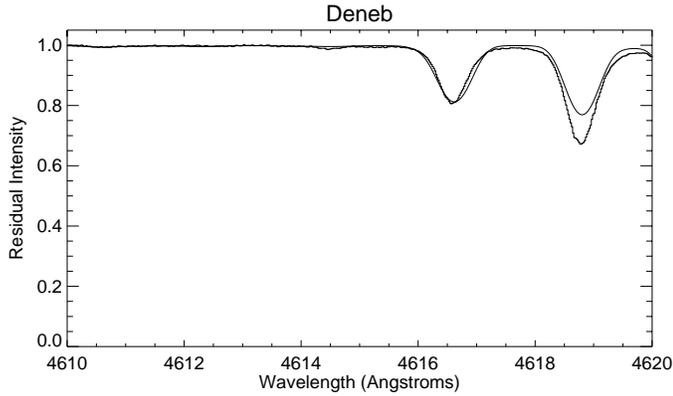
Fig. 7. A sample section for $\lambda\lambda 4610$–4620 of the observed spectrum of Deneb (broken line) compared with a synthetic spectrum using the results of the fine analysis.
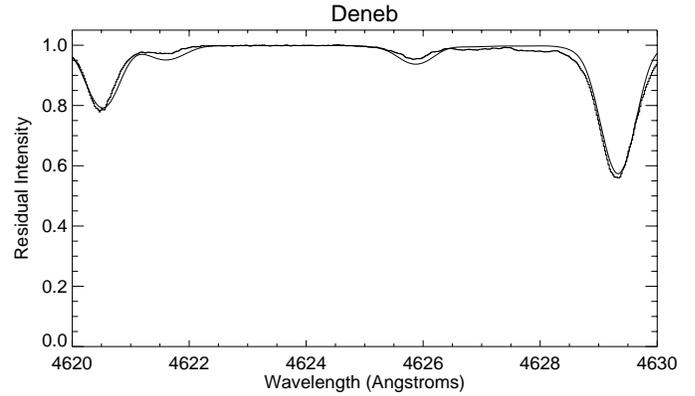
Fig. 8. A sample section for $\lambda\lambda 4620$–4630 of the observed spectrum of Deneb (broken line). Otherwise, the same as in Fig. 7.

Table 5. Values of microturbulence velocity (ξ) for some elements found by different authors in the atmosphere of Deneb.

Species	ξ (km s^{-1})			
	Rosendhal (1970)	Zverko (1971)	Aydın (1972)	This Study
Mg I	...	...	...	3.60
Mg II	...	...	...	6.50
Si II	...	...	...	8.50
Ti II	10.50	11.00	10.64	8.00
Cr II	...	...	10.00	11.90
Fe I	...	...	5.33	3.60
Fe II	11.80	17.00	11.94	10.40

can be used to produce a spectrum which is similar to the observations.

5. Comparison to other analyses

5.1. Microturbulence

The microturbulence values for Deneb are 3.60, 6.50, 8.50, 8.00, 11.90, 3.60, and 10.40 km s^{-1}, respectively, for Mg I, Mg II, Si II, Ti II, Cr II, Fe I, and Fe II lines. The microturbulence is different from one element to another and for neutral and singley ionized magnesium and iron lines. Aydın (1972) found that there is a relation between the microturbulence values for various ions in the atmosphere of Deneb and other A-type supergiants, such that ξ(Fe II) > ξ(Ti II, Cr II) > ξ(Fe I). His study yields the values for the microturbulence in the range of 5 to 12 km s^{-1} for Deneb with 10.64, 10.00, 11.94 and 5.33 km s^{-1}, respectively, for Ti II, Cr II, Fe II, and Fe I. Rosendhal (1970) found 10.5 and 11.8 km s^{-1} and Zverko (1971) gave 11.0 and 17.0 km s^{-1}, respectively, for Ti II and Fe II lines (Table 5). The previously determined values of microturbulence for Ti II, Fe II and Fe I are greater than the values found here for these species, while Aydın's value for Cr II is less than the value found here. The persistence of the atomic species dependent microturbulent velocies in the equivalent widths found here, as in the earlier results, may imply their reality. This suggests a variation of microturbulent velocity

with height in the atmosphere as was previously reported for Deneb (Groth 1961; Rosendhal 1970; and Samedov 1993).

De Jager et al. (1984) and Boer et al. (1988) calculated the local velocity of sound to be 14 and 8–12 km s^{-1} in Deneb, respectively, close to their microturbulent velocities of 15.0 and 10.3 km s^{-1}. The velocity field can be described by propagating sound waves in the outer part of the photosphere in this star. They subsequently concluded that sound waves can turn into shock waves which are a dominant structure in the atmosphere of Deneb. Also, Samedov (1993) determined the speed of sound for Deneb and found that supersonic microturbulence develops in the upper layers of the atmosphere. We have calculated the mean velocity of sound to be 15 km s^{-1} (with $\gamma = 5/3$, T = T$_{\text{eff}}$ and $\mu = 0.53$). The value is in good agreement with De Jager et al. (1984)'s value while Boer et al. (1988)'s value is a little smaller than ours.

5.2. Helium abundance

Our analysis of eight He I lines indicated a slightly under-abundance of helium by 0.15 dex (log ϵ(He) = 10.85 $\pm$ 0.01 in Sect. 3.2). The helium abundances from five spectral lines derived by Samedov (1993) for Deneb is 11.30 $\pm$ 0.10, which is about 0.45 dex larger than our determination. Samedov's W$_\lambda$ values are about 170% and 320% larger than ours for his lines. Measuring the equivalent widths of He I lines is difficult as the profile can be more complicated than a Gaussian one, especially for triplet lines. It is better to match profiles after proper convolution of the model results with the rotational and instrumental profile. Groth et al. (1992) reported a nearly normal He abundance (log ϵ(He) $\sim$ 11.0) for Deneb with model parameters similar to those of Groth (1961) (see Albayrak 1999). Takeda et al. (1996) found an NLTE helium abundance for Deneb log ϵ(He) = 10.85, with model parameters T$_{\text{eff}}$ = 9000 K, log g = 1.5 similar to our results of T$_{\text{eff}}$ = 9000 K, log g = 1.45 in agreement with this LTE study.

Kudritzki (1973) showed that the helium abundances affect the atmospheric structure of A-type supergiants. An increase in the helium abundance changes the mean molecular weight of a column gas in the atmosphere, which decreases the

amount of opacity per gram of gas and modifies the pressure stratification. The results are larger hydrogen discontinuities and stronger hydrogen lines, similar to the effects of increasing gravity. Humphreys et al. (1991) demonstrated that hydrogen line strengths and discontinuities of a group of A-type supergiants are too strong for their high luminosities, and therefore they have anomalous *UBV* colors. They concluded that this effect is the result of an extreme helium enrichment in the stellar atmosphere. But Deneb is He poor, it is a more normal A-type supergiant.

5.3. CNO abundances

We have found an underabundance of C (by 0.34 dex), an overabundance of N (an average of 0.63 dex), and O (by 0.25 dex) for Deneb with respect to the Sun. The abundances of C and O in Deneb determined by Groth et al. (1992) are $\log \epsilon(C) = \log \epsilon(O) = 8.04$ that results in a significant C (0.51 dex) and O (0.84) deficiency relative to the Sun. The abundances of N, C, and O in Deneb determined by Samedov (1993) are a large excess of 1.11 dex, and deficit of 0.32 and 0.17 dex, respectively. Also, Takeda et al. (1996) determined CNO abundances of Deneb from NLTE analysis and concluded that C is conspicuously underabundant by ~ 0.80 dex, N shows a moderate excess of 0.30 dex, and O seems to be deficient by ~ 0.30 dex. Table 6 gives the CNO abundance results derived by different authors for Deneb.

Recently, Venn (1995b) studied LTE CNO abundance of 22 A-type supergiants the luminosity range from Ia to II, but not including Deneb. Also, effects of departures from LTE on the carbon and nitrogen abundance for these stars were determined. For carbon, NLTE corrections for the cooler supergiants that range from –0.10 in the F0 stars to –0.50 dex in the A3 stars (from 14 sample supergiant stars) were found. Furthermore, for the eight sample supergiants in the spectral range from A0 to A2, it was concluded that NLTE carbon abundance corrections are unreliable as the results give extremely low NLTE C abundances.

We derived carbon (C I) abundances from three lines of $W_\lambda \leq 4$ mÅ which form deep in the atmosphere ($\log \tau = 0.28$) where LTE is usually a sufficient description. Since overionization occurs mostly in the upper layers of the atmosphere, using those lines with high excitation potentials (i.e., lines that form deeper in the atmosphere) minimizes the effect.

The average LTE carbon abundances derived by Venn (1995b) for these eight early A-type supergiant atmospheres is $\langle \log \epsilon(C/H) \rangle = 8.18 \pm 0.22$ and is similar to our determination for Deneb which is 8.21 ± 0.20.

For the NLTE correction of nitrogen, Venn (1995b) also finds values ranging from –1.0 in the A0 stars to –0.30 dex in the F0 stars (from 22 sample supergiant stars). It was suggested that the NLTE nitrogen abundances are roughly solar for all the A-type supergiants examined. Luck & Lambert (1985) found that departures from LTE could enhance the N I lines in the A supergiant atmospheres and concluded that the correction for the lines formed in deep layers is near zero, but corrections as large as –1.0 dex were found for the lines formed in high layers.

Table 6. The derived CNO abundances for Deneb by different authors ($\log \epsilon$).

Species	Groth (1961)	Groth et al. (1992)	Samedov (1993)	Takeda et al. (1996)	This Work
C	8.12	8.04	8.35	7.83	8.21
N	9.33	8.04	9.10	8.30	8.59
O	7.29	...	8.75	8.52	8.63

Furthermore, recently Takeda et al. (1996) found an NLTE nitrogen excess of 0.30 dex for Deneb. Their result is expected to be more applicable to Deneb. Firstly, Takeda et al. (1996) derived this result from the atmospheric analysis of Deneb. Secondly, their atmospheric parameters ($T_{\rm eff} = 9000$ K, $\log g = 1.50$) are very similar to ours ($T_{\rm eff} = 9000$ K, $\log g = 1.45$). On the other hand, the departures from LTE for C I, N I and O I lines were calculated by Takeda & Takeda-Hidai (1995) from the Luck & Lambert (1985)'s data set for four F supergiants (α Car, ι Car, α Lep, and α Per) and from Venn (1993)'s data set for three A-supergiants (η Leo, 13 Mon, and HD 13476). Their results show that the NLTE corrections are not important for lines of C I and O I ($W_\lambda < 10$ mÅ). Also, one can see in their Tables 5 and 6 that NLTE corrections become small for the lines formed in deeper layers.

NLTE effects cannot be ruled out as the source of the extreme nitrogen enhancements calculated here for Deneb. However, we include the lines of $W_\lambda \leq 10$ mÅ for the abundance calculation of this species which formed rather deep in the atmosphere ($\log \tau = 0.30$). Therefore, the results of our LTE analysis for C, N, and O are not significantly overestimated due to the neglect of NLTE corrections.

5.4. Light element abundances (Mg to Ca)

Table 7 lists light element abundances found by different authors in Deneb. The Mg I/II abundances ([Mg/H] = +0.02) are in excellent agreement with solar within the error limits. For our ionization equilibrium determination using Mg I and Mg II lines (and also Fe I and Fe II, discussed above), we require that $\log \epsilon(Mg I) \sim \log \epsilon(Mg II)$, without any constraint on the Mg abundance (and Fe) in this calculation. Groth et al. (1992) concluded that a Mg abundance which is $\log \epsilon(Mg) = 7.79$ is in fairly good agreement with our result ($\log \epsilon(Mg) = 7.60$) considering differences in the atmospheric parameters. Samedov (1993) determined the magnesium abundance as an excess of 0.37 dex ($\log \epsilon(Mg) = 7.97$) from the average of only two Mg II lines. But his W_λ measurements for these Mg lines ($\lambda 3848.24$ and $\lambda 4851.10$) are 57 and 37 mÅ while the measurements here are 48 and 9 mÅ, respectively. For Mg II $\lambda 4851.10$ $\log gf = -2.22$ dex was adopted while –0.68 dex was used here. The other disagreements came from differences in the atmospheric parameters. Venn (1995a) found an LTE average abundance of $\langle \log \epsilon(Mg) \rangle = 7.47$, for the sample supergiants (the spectral range A0 to F0 and luminosity range Ia to II) which is fairly good agreement with our value (see Table 9).

Table 7. The derived light element abundances by different authors for Deneb (log ϵ).

Species	Groth (1961)	Samedov (1993)	Takeda et al. (1996)	This Work
Mg I	7.81	...	...	7.69
Mg II	7.67	7.97	...	7.51
Al I	6.52	...	...	6.25
Al II	...	...	...	6.21
Si II	7.81	7.95	...	7.40
S II	...	...	7.63	6.90
Ca II	6.40	...	...	6.79

Table 8. The derived iron peak element abundances by different authors for Deneb (log ϵ).

Species	Groth (1961)	Samedov (1993)	This Work
Sc II	3.12	2.90	2.95
Ti II	5.06	5.10	5.00
V II	3.81	4.37	4.12
Cr I	6.50	...	6.06
Cr II	5.60	5.66	5.72
Mn I	5.50	...	5.36
Mn II	...	...	5.60
Fe	7.55	7.83	7.65
Ni I	...	...	6.48
Ni II	4.75	6.50	6.24

Table 9. Comparison of the results of this study with those of Venn (1995a).

Species	# Stars	$\langle \log \epsilon_\star \rangle$	Deneb	[x]
Mg I	19	7.48 ± 0.17	7.69 ± 0.26	0.21
Mg II	22	7.46 ± 0.17	7.51 ± 0.14	0.05
Si I	11	7.48 ± 0.14	...	...
Si II	5	7.83 ± 0.17	7.40 ± 0.21	0.07
S I	7	7.55 ± 0.15	6.90 ± 0.25	–0.65
Ca I	15	6.65 ± 0.19	...	...
Ca II	10	6.03 ± 0.26	6.79	0.76
Sc II	9	3.13 ± 0.20	2.95 ± 0.18	–0.18
Ti II	22	4.86 ± 0.25	5.00 ± 0.23	0.14
Cr I	8	5.89 ± 0.10	6.06 ± 0.19	0.17
Cr II	18	5.61 ± 0.23	5.72 ± 0.29	0.11
Mn II	16	5.81 ± 0.20	5.60 ± 0.27	–0.21
Fe I	22	7.56 ± 0.24	7.74 ± 0.30	0.01
Fe II	22	7.40 ± 0.11	7.57 ± 0.27	0.17
Ni I	11	6.35 ± 0.15	6.48 ± 0.21	0.13
Ni II	...	...	6.24 ± 0.08	...
Sr II	4	2.41 ± 0.21	3.28 ± 0.09	0.87
Zr II	3	2.81 ± 0.06	3.41 ± 0.20	0.60

[x]= Deneb – Venn's result

The aluminium abundances previously determined only by Groth (1961) from two Al I lines of $\lambda3944$ and $\lambda3961$ in Deneb of log ϵ(Al I) = 6.50 and 6.54 using gf-values of –0.58 and –0.28 dex respectively, implies an average excess of ~ 0.50 dex to solar. Our values are log ϵ(Al I) = 6.31 and 6.13 with gf-values of –0.64 and –0.34 dex respectively, and implies an average deficient of 0.22 dex. His W_λ value is 20% larger than that found here for $\lambda3961$ while the other lines W_λ is the same. The differences are due to substantial changes in the atomic oscillator strength and the adopted model atmosphere. Our result for aluminium indicates a slight subsolar abundance by ~ 0.24 dex.

The Si abundance shown here, log ϵ(Si) = 7.40 ± 0.21, from eleven lines, is in good agreement with the solar abundance. Samedov (1993) found an excess of 0.40 dex from two lines ($\lambda3853.66$ and $\lambda4130.89$). The difference comes from his W_λ measurements, his gf-values of –1.61 and 0.46 dex while the values here are –1.44 and 0.53 dex for these lines respectively, and atmospheric parameters are T_{eff} = 9100 K, log g = 1.20. Venn (1995a)'s derived average LTE abundances of $\langle \log \epsilon(\text{Si}) \rangle$ = 7.40 for the sample supergiants is in very good agreement with the value found here (see also Table 9).

My sulfur abundance, determined from ten lines, is underabundant by ~ 0.43 dex. Takeda et al.(1996)'s NLTE analysis yields an overabundance of 0.40 dex, but is derived from only one line. Also, Venn found that $\langle \log \epsilon(\text{S}) \rangle$ is an excess of 0.28 dex from the sample of supergiants.

The Ca II abundance in this analysis is from only one line and yields an appreciable overabundance of 0.43 dex. Groth (1961) found for this element an excess of 0.30 dex in Deneb. Venn (1995a) derived $\langle [\text{CaI/H}] \rangle$ = 0.31 and $\langle [\text{CaII/H}] \rangle$ = –0.31 dex for the sample stars. Hence Ca I yields lower (while Ca II yields greater) Ca abundances than solar.

5.5. Iron group element abundances (Sc to Ni)

Since the progenitor stars are more massive than the Sun, one may expect some small enrichment in the metal abundances for normal Population I supergiants due to Galactic chemical evolution. We find the metal abundances (the results of iron group elements, Sc to Ni, are given in Table 8 with those previously determined) tend to be greater than solar for Deneb.

Our Sc and Ti abundances are in good agreement with solar and with the derived values of Samedov (1993), but for these elements his W_λ measurements and the adopted gf-values are different from ours.

The mean log ϵ(V) value from 21 lines for Deneb is 4.12 ± 0.28, which indicates that its derived abundance is close to solar, more nearly solar than the value of Samedov (1993), 4.37 ± 0.06 (from 5 lines).

Abundances from Cr I and Cr II lines differ by 0.34 dex. The Cr I abundances are from only 6 lines and yield greater abundances than solar. The Cr II abundances are from 49 lines and yield nearly solar abundance. Both species show the same trend in abundance analysis determined by Venn (1995a) for supergiants (Table 9). This table lists the abundances determined in this study for Deneb, the mean abundances determined by Venn for a selection of A-type supergiants, differences between the abundance results of these two studies.

Mn is an overabundance of 0.21 dex. Venn (1995a) found for this species an average excess of 0.42 dex for 16 A supergiants (see Table 9).

Abundances from Fe I and Fe II lines are often in agreement. To determine the atmospheric parameters of Deneb we have also used the ionization equilibrium of the Fe I/II lines (discussed in Sect. 3.1). Also, we consider this element a good indicator of the overall metalicity in Deneb as there are a large number of Fe I and II lines available (see Table A.1 in appendix). Our mean derived abundance of iron (log ϵ(Fe) = 7.65) in Deneb is overabundant by 0.15 dex while Samedov (1993)'s result from six lines (log ϵ(Fe II) = 7.83) is overabundant by 0.33 dex (the differences mainly come from his W_λ measurements and the *gf*-values). The abundance derived in this study for Fe is in agreement with that derived by Venn (1995a).

The abundance of Ni appears to be marginally high (~ 0.11 dex) relative to solar in Deneb while for 11 A supergiants it is an excess of 0.10 dex as found by Venn (1995a). Samedov (1993) determined log ϵ (Ni II) = 6.50 ± 0.07 from four lines in Deneb (greater by 0.26 dex than ours).

5.6. Heavy (Sr, Y and Zr) rare-earth (Ba, La and Eu) element abundances

Our derived abundance of strontium for Deneb, which is greater than solar by 0.31 dex, is based on the two Sr II resonance lines. Samedov's (1993) result from these lines is almost solar. His adopted *gf*-values are typically 0.06 to 0.21 dex larger. Also, Groth (1961) reported an overabundance by 0.54 dex. Venn (1995a) concluded that Sr abundances in four early A-type supergiants show an average underabundance of 0.52 dex. Y, Zr, Ba, La and Eu abundances have not been previously determined in Deneb. The Y abundance has been calculated from five lines. The Zr abundance is based on 12 lines while Ba, La and Eu abundances came from only one line each. The Y, Zr and Ba are significantly overabundant while the La and Eu are extremely overabundant. Overabundances of Zr (on the average of 0.21 dex) have also been reported by Venn (1995a) in three supergiants.

Mashonkina et al. (private communication) performed NLTE strontium abundance for Deneb using our data (W_λ) for Sr II $\lambda4077$ and $\lambda4215$ and the atmospheric parameters of this study. They found an NLTE strontium excess of 0.51 and 0.71 dex in Deneb for these lines, respectively. Thus, their NLTE results give an overabundance of Sr amounting to 0.61 dex while the LTE overabundance is 0.31 dex. Further, Belyakova et al. (2000) calculated NLTE strontium abundances for A-type stars and concluded that Sr is overabundant in normal A-stars. Hence, the overabundance of Sr obtained for Deneb seems to be typical for A-stars.

6. Evolutionary status

The evolutionary status of normal Galactic A-type supergiants can be determined from the CNO contents of their atmospheres. If a massive (5–40 $M_\odot$) star evolves quickly off the main se-

quence to the red giant branch, then the development of a deep surface convection zone, mixes gas from hydrogen-burning layers to the outer observable layers, a process known as the first dredge-up. Hydrogen burning on the main sequence primarily occurs via the CNO-cycle in these stars, thus the surface abundances of carbon, nitrogen and oxygen will be altered (C decreased, N enriched and O slightly reduced) with the sum of the nuclei remaining constant since they only act as catalysts in the CNO tri-cycle. According to an alternative scenario, these stars initiate helium core burning without visiting the red giant branch. Hence, they would evolve directly from the main sequence (Stothers & Chin 1976; Stothers & Chin 1991; Chiosi & Summa 1970; Iben 1966). In this scenario, a fully convective intermediate zone is predicted, such that after He ignition, the envelope is able to establish thermal equilibrium without rapid expansion. Therefore, the star is stable as an A-type supergiant when core He burning begins, and in this case, no mixing with deeper layers is anticipated, hence the CNO abundances should be normal. If these stars are post-red giant stars, then CNO will resemble the first dredge-up abundance pattern. A more detailed discussion of the predictions of evolution of A-type supergiants is given by Venn (1995b, and references therein).

Also, Venn (1995a, b) determined abundances of metals, carbon, nitrogen and oxygen for a selected group of supergiants (the spectral range from A0 to F0 and the luminosity range from Ia to II), but not including Deneb. This examined the NLTE correction to the carbon and nitrogen abundances and suggested that these supergiants have not undergone the first dredge-up, but that only some partial mixing with CNO-cycled layers has occurred in these stars. Therefore, it was concluded that A-type supergiants have evolved directly from the main sequence without visiting red giant branch. Recently, abundances of boron have been determined by Venn et al. (1996) from IUE spectra of the B II line at $\lambda1362$ for two early A-type supergiants 13 Mon (A0 Ib), and η Leo (A0 Ib) as log ϵ(B) = 0.0 ± 0.5 and 0.5 ± 0.3, respectively. The meteoritic abundance of boron is log ϵ(B) = 2.79 ± 0.05 Grevesse et al. (1996). Thus boron is only moderately depleted in these supergiants, suggesting only a partial mixing.

Our abundances of carbon, nitrogen, and oxygen for Deneb are different from solar. The carbon abundance is 8.21 (a deficient of 0.34 dex), the nitrogen is 8.88 (an overabundance of 0.91 dex from N I lines), and the oxygen is 8.63 (an underabundance of 0.25 dex). This abundance signature suggests CNO cycling, where the surface abundances have been mixed with CNO-processed gas prior to its current supergiant stage. If CNO-cycling is responsible, then the sum of the CNO nuclei will be constant as its initial composition. We find using log ϵ(N) = log ϵ(N I) that [(C+N+O)/Fe] is –0.02 for Deneb which, within the uncertainties of the analysis, indicates that the total number of atoms has not changed from an initially solar composition. Also, other CNO analyses of early A-type supergiants: the study by Lambert et al. (1989) of η Leo (A0 Ib), by Ivanova & Lyubimkov (1990) of σ Cyg (B9 Iab), by Tomkin & Lambert (1994) of ξ^1 Sgr (A0 II), indicated deep mixing. Lennon & Dufton (1986) determined the surface abundance of HD 148379

(B1.5 Ia) and HD 157038 (B3 Ia) and suggested that HD 157038 evolved through a red supergiant phase.

If Deneb is a typical supergiant to which there is no contrary argument, then it too must have passed through a dredge-up stage, i.e. one of deep mixing. From Table 3, we also find the average [s-process elements/Fe] where s-process elements from Sr to La are enriched by 0.47 dex in Deneb. If Ba and La are omitted, [s-process elements/Fe] = 0.42 which is slightly less. So, what is the reason for large overabundances of Sr, Y, Zr, Ba, La, and Eu? This is a subject for stellar evolutionary theory to investigate.

7. Conclusions and final comments

1. From 35 independent sets of radial velocity values, the maximum and minimum observed values are +3.35 and –11.51 $\mathrm{km\,s^{-1}}$ respectively, with a maximum range of 14.86 $\mathrm{km\,s^{-1}}$ (see Albayrak et al. 2000). This is in good agreement with the derived macroturbulence velocity of 14 $\mathrm{km\,s^{-1}}$. As a characteristic of early type Ia supergiants (Abt 1957), Deneb shows quasi-periodic variations of radial velocity (Paddock 1935) due to multiperiodic nonradial oscillations (Lucy 1976).
2. The projected rotational velocity $v \sin i = 25\,\mathrm{km\,s^{-1}}$, is close to Abt & Morell (1995)'s value of 30 $\mathrm{km\,s^{-1}}$.
3. The effective temperature and surface gravity of Deneb were determined as compromise values, $T_{\mathrm{eff}} = 9000$ K and log $g = 1.45$, using Mg I/II and Fe I/II ionization equilibrium, and comparison of the observed continuum flux and the H_γ profile with values calculated using ATLAS9 models which assumed a solar composition.
4. The microturbulent velocities found from individual atomic species range from 3.60 to 11.90 $\mathrm{km\,s^{-1}}$. There are significant differences between microturbulent velocities found for neutral and singly ionized magnesium and iron lines and also a clear variation of microturbulence with species. The simplest interpretation of these results is that they may represent a stratification effect and may reflect the existence of a velocity gradient in the atmosphere of this star. Similar results have been reported in the past for Deneb (Rosendhal 1970, Zverko 1971, and Aydın 1972).
5. The abundances of Deneb are quite similar to those of other A-type supergiants. Helium is underabundant by 0.15 dex. There is a large enrichment of nitrogen ([N/H] = +0.63), accompanied by slight carbon ([C/H] = –0.34) and possibly oxygen depletion ([O/H] = –0.25). These results and the sum (C+O+N) are consistent with the predictions for CNO-processed envelopes of post red supergiants stars that have undergone the first dredge-up mixing event. Aluminium and sulfur appear to be underabundant. The magnesium and silicon abundances are solar. This is only a small enrichment in the metal abundances (Ca to Ni) for Deneb relative to the Sun, but no overall metal enrichments are determined in this analysis. Our result is consistent with the study by Venn (1995a) who derived metal abundance for 22 A-type supergiants. Deneb is strontium, yttrium and zirconium overabundant and is also barium, lanthanum and europium rich although these abundances are based each on only one line.

Appendix

The analyses of all line data for Deneb in Table A.1 are only available with the on-line publication at http://link.springer.de/link/service/journals/00230. The lines are sorted according to species; multiplet number, wavelength, the *gf*-value with its source, and the deduced abundance are listed. Equivalent widths are given per line in milliangstroms. Spectral lines that are significantly blended with other elements have not been included.

References

Abt H.A., 1957, ApJ 126, 138

Abt H.A., Morrell N.I., 1995, ApJS 99, 135

Adelman S.J., Pyper D.M., Lopez-Garcia Z., Çalışkan H., 1995, A&A 296, 472

Albayrak B., 1999, Ph.D. Thesis, Ankara University, Graduate School of Nature and Applied Sciences, Department of Astronomy and Space Sciences, Ankara, Turkey

Albayrak B., Adelman S.J., Gulliver A.F., et al., 2000, in preparation

Alekseeva G.A., Arkharov A.A., Galkin V.D., et al., 1996, Baltic Astronomy 5, 603

Aydın C., 1972, A&A 19, 369

Belyakova E.V., Mashonkina L.I., Sakhibullin N.A., 2000, in preparation

Biémont E., Grevesse N., Hannaford P., Lowe R.M., 1981, ApJ 248, 867

Biémont E., Karner C., Meyer G., Trager F., zu Putlitz G., 1982, A&A 107, 166

Biémont E., Grevesse N., Faires L.M., et al., 1989, A&A 209, 391

Boer B., De Jager C., Nieuwenhuijzen H., 1988, A&A 195, 218

Breger M., 1976, ApJS 32, 7

Buscombe W., 1951, ApJ 114, 73

Chadeau C., 1955, Ann. d'Ap. 18, 100

Chiosi C., Summa C., 1970, Ap&SS 8, 478

Cowley C.R., Corliss C.H., 1983, MNRAS 203, 651

De Jager C., Mulder P.S., Kondo Y., 1984, A&A 141, 304

Fitzgerald M.P., 1970, A&A 4, 234

Fuhr J.R., Martin G.A., Wiese W.L., 1988, J. Phys. Chem. Ref. Data 17, Suppl. 4

Fuhr J.R., Wiese W.L., 1990, In: Lide D.R. (ed.) CRC Handbook of Chemistry and Physics. CRC Press, Cleveland, Ohio

Gigas D., 1986, A&A 165, 170

Gigas D., 1988, A&A 192, 264

Gray R.O., 1992, A&A 265, 704

Grevesse N., Biémont E., Hannaford P., Lowe R.M., 1981, In: Upper Main Sequence CP Stars. 23rd Liège Astrophys. Colloq., Universitè de Liège p. 211

Grevesse N., Noels A., Sauval A.J., 1996, In: Holt S.S., Sonneborn G. (eds.) Cosmic Abundances. ASP Conference Series, p. 117

Groth H.G., 1961, Z. Astrophys. 51, 206

Groth H.G., Kudritzki R.P., Butler K., Humphreys R.M., 1992, In: Heber U., Jeffery C.S. (eds.) Atmospheres of Early-Type Stars. Lecture Notes in Physics, p. 53

Gulliver A.F., Hill G., Adelman S.J., 1994, ApJ 489, L81

Gulliver A.F., Hill G., Adelman S.J., 1996, In: Adelman S.J., Kupka F., Weiss W.W. (eds.) Model Atmospheres and Spectrum Synthesis. ASP Conference Series p. 232

Hannaford P., Lowe R.M., Grevesse N., Biémont E., 1982, ApJ 261, 736

Hayes D.S., Latham D.W., 1975, ApJ 197, 593

Heise H., 1974, A&A 34, 275

Hill G., Adelman S.J., 1986, In: Cowley C.R., Dworetsky M.M., Méssegier C. (eds.) Upper Main Sequence Stars with Anomolues Abundances. Reidel, Dordrecht, Holland, p. 209

Hill G., Fisher W.A., 1986, Publ. Dominion Astrophys. Obs. 16, No. 13

Hubeny I., Lanz T., Jeffery C.S., 1994, Daresbury Lab. New. Anal. Astron. Spectra No. 20, p. 30

Humphreys R.M., Kudritzki R.P., Groth H.G., 1991, A&A 245, 593

Iben I. Jr., 1966, ApJ 143, 516

Ivanova Z.K., Lyubimkov L.S., 1990, Bull. Crimean Astrophys. Obs. 79, 45

Jönsson G., Kröll S., Persson A., Svanberg S., 1984, Phys. Rev. A. 30, 2429

Kubat J., 1996, In: Adelman S.J., Kupka F., Weiss W.W. (eds.) Model Atmospheres and Spectrum Synthesis. ASP Conference Series, p. 165

Kudritzki R.-P., 1973, A&A 28, 103

Kurucz R.L., Peytremann E., 1975, SAO Special Report, 362

Kurucz R.L., 1979, ApJS 40, 1

Kurucz R.L., Avrett E.H., 1981, Smithsonian Astrophys. Obs. Spec. Rep., 391

Kurucz R.L., 1995, In: Adelman S.J., Wiese W.L. (eds.) Astrophysical Applications of Powerful New Databases. ASP Conference Series, p. 205

Kurucz R.L., Bell B., 1995, Kurucz CD-ROM No. 23, Atomic Line List. Harvard-Smithsonian Center for Astrophysics, Cambridge

Lambert D.L., Hinkle K.H., Luck R.E., 1989, ApJ 333, 917

Lamers H.J.G.L.M., Achmad L., 1994, A&A 291, 856

Lanz T., 1986, Photoelectric Photometric Catalogue in the Johnson UBVRI System. ST Systems Corporation, Lanham, Maryland

Lanz T., Artru M.-C., 1985, Phys. Scripta, 32, 115

Lawler J.E., Dakin J.T., 1989, JOSA B, 6, 1457

Lennon D.J., Dufton P.L., 1986, A&A 155, 79

Luck R.E., Lambert D.L., 1985, ApJ 298, 782

Lucy L.B., 1976, ApJ 206, 499

Magazzu A., Cowley C.R., 1986, ApJ 134, 562

Martin G.A., Fuhr J.R., Wiese W.L., 1988, J. Phys. Chem. Ref. Data 17, Suppl. 3

Mashonkina L.I., Shimanskaya N.N., Shimansky V.V., 1995, In: Adelman S. J., Wiese W.L. (eds.) Astrophysical Applications of Powerfull New Databases. ASP Conference series, p. 389

Meynet G., Hauck B., 1985, A&A 150, 163

Mermilliod J.C., 1991, Photoelectric Photometric Catalogue of Homogeneous Measurements in the UBV System. Institut d'Astronomie, Universite de Lausanne, CH-1290 Chavannes-des-Bois, Switzerland

Moore C.E., 1945, A Multiplet Table Astrophysical Interest. Princeton University Observatory

Paddock G.F., 1935, Lick. Obs. Bull. 17, 49

Rosendhal J.D., 1970, ApJ 160, 627

Rufener F., 1976, A&AS 26, 275

Samedov Z.A., 1993, AZh 70, 82

Schild R., Peterson D.M., Oke J.B., 1971, ApJ 166, 95

Schild R.E., 1977, AJ 82, 337

Schulz-Gulde E., 1969, J.Q.S.R.T. 9, 13

Stothers R.B., Chin C., 1991, ApJ 204, 472

Stothers R.B., Chin C., 1976, ApJ 381, L67

Taffara N.S., 1966, Mem. Soc. Astron. Ital. 37, 401

Takeda Y., Takada-Hidai M., 1995, PASJ 47, 169

Takeda Y., Takada-Hidai M., Kotake J., 1996, PASJ 48, 753

Tomkin J., Lambert D.L., 1994, PASP 106, 365

Venn K.M., 1993, ApJ 414, 316

Venn K.M., 1995a, ApJS 99, 659

Venn K.M., 1995b, ApJ 449, 839

Venn K.M., Lambert D.L., Lemke M., 1996, A&A 307, 849

Verdugo E., Talavera A., Gomez de Castro A.I., 1999, A&A 346, 819

Ward L., 1985, MNRAS 213, 71

Wiese W.L., Smith M.W., Glennon B.M., 1966, NSRDS-NBS 4, US Government Printing Office, Washington DC

Wiese W.L., Smith M.W., Miles B.M., 1969, NSRDS-NBS 22, US Government Printing Office, Washington DC

Wiese W.L., Martin G.A., 1980, NSRDS-NBS 68, Part 2, US Government Printing Office, Washington DC

Wiese W.L., Fuhr J.R., Deters T.M., 1996, J. Phys. Chem. Ref. Data, Monograph 6

Zverko J., 1971, Bull. Astron. Inst. Czech. 22, 49